University Turbine System Research (UTSR)
2017 Gas Turbine Industrial Fellowship Program

Final Report

Prepared for:

Siemens Energy
Orlando, FL

&

Southwest Research Institute
San Antonio, TX

Prepared By:
Lincoln DiLorenzo
Montana State University
Mechanical Engineering
Bozeman, MT

Introduction

Additive manufacturing (AM) has become an increasingly attractive method of manufacturing gas turbine components such as blades or vanes. One reason for this is the absence of design limitations and constraints that are present when dealing with modern, conventional manufacturing methods. The absence of these limitations can allow for new designs and features to be implemented in components potentially leading to improvements in overall thermal efficiency and power output of gas turbines.

Siemens has been a key player in advancing and applying AM technology, especially in the gas turbine industry. Siemens recently announced performing successful full load engine tests for the first time using gas turbine blades that were produced entirely using AM. The blades were made with both a conventional design as well as a new design with improved cooling features. A blade produced with AM can be seen in Figure 1.

Figure 1: Turbine blade produced with AM for full load engine tests [1]

The blades were installed in an SGT-400 industrial gas turbine and experienced 13000 RPM and temperatures exceeding 1250 °C [1]. The team behind this project was able to complete everything from start to finish in 18 months [1], a relatively short amount of time for turbine blade design and manufacture. This shows another promising aspect of AM, the speed at which AM allows things to be done. The success of the tests validates the use of AM in turbine components and has pushed Siemens to continue to innovate and advance AM technology. In addition to manufacturing turbine blades, Siemens has utilized AM to produce burner tips and nozzles as well as repairing burner heads [2].

The work performed during the 12 week fellowship was designed to aid a team of Siemens engineers in Orlando, Florida tasked with applying AM to gas turbine components. Two main projects were worked on throughout the fellowship: information collection and heat transfer validation. The contents of this report will discuss both projects but will focus mainly on the heat transfer validation.

Information Collection

Throughout the course of the fellowship, information regarding AM applied to gas turbine components, specifically blades, vanes, and ring segments, was collected and organized. A patent database was browsed to collect over 60 patents filed by engineers from Siemens as

well as its competitors such as General Electric, United Technologies Corp, and others innovating in the field of additive manufacturing. An additional 49 patents were received to resulting in over 110 patents. The patents were grouped together in the following categories:

- Blade
- Vane
- Ring Segment
- Other Components
- Repair
- Material composition
- AM process/system

These patents were then uploaded to a database accessible by Siemens engineers resulting in a centralized location for patents regarding AM applied to gas turbine components.

In addition to the patent search, internal lessons and summaries were collected from key technical leads of projects occurring throughout Siemens. Due to the confidential nature of this information, no further discussion of this material will be included in this report.

Heat Transfer Validation

Introduction

Achieving gains in gas turbine efficiency and power output has been a topic of great importance for those involved in the power generation industry. Increasing the turbine inlet temperature has been one way that has been explored to achieve these gains. Current turbine inlet temperatures already surpass the melting temperature of the super alloy metals that were used to manufacture the turbine components. To allow operation at these high turbine inlet temperatures, the turbine components must be cooled. This cooling has typically been achieved through bulk, or macro, cooling features such as serpentine passages, impingement jets, or pin banks. As advances in AM technology have been developed and demands for improved and higher levels of cooling are needed, the idea of micro cooling has become a possible solution.

As discussed in Bunker [3], the main geometric attributes of micro cooling are that the cooling network is made up of smaller, highly distributed channels that are closer to the outer surface of the airfoil when compared to macro cooling. This design provides for better uniformity of cooling and lesser in-plane thermal gradients as well as a more efficient transfer of energy as heat [3]. AM can play a role in the push towards micro cooling by allowing the creation of these smaller, complex cooling networks that could not be manufactured previously.

Interest in Bunker was stirred up due to the promising improvements that can result from micro cooling, however some simple back calculations from Siemens engineers showed some uncertainties in the numbers presented in Bunker. This portion of the report will summarize the work done to replicate the heat transfer analysis of a simplified airfoil wall section performed in Bunker and either validate or debunk the conclusions made. The setup of the work is documented in Bunker and will be included in this report by reference.

Results

Bulk Cooling

The bulk cooling portion of the calculations was done in an Excel spreadsheet. A series composite wall for the one dimensional heat transfer analysis was drawn to represent the simplified airfoil wall section and can be seen Figure 2.

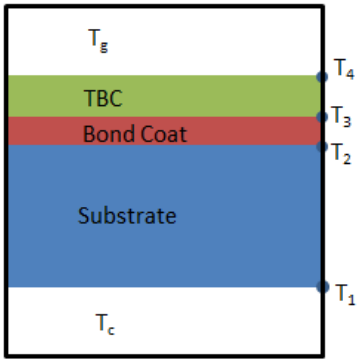

Figure 2: Simplified wall section of an airfoil representing a bulk cooling scheme

Using a thermal circuit to represent the composite wall, the heat flux through the entire wall section was defined as

$$q" = \frac{T_g - T_c}{\frac{1}{h_g} + \frac{t_{tbc}}{k_{tbc}} + \frac{t_{bond}}{k_{bond}} + \frac{t_s}{k_s} + \frac{1}{h_c}} \tag{1}$$

With the heat flux known, temperature 4 was calculated using the convection equation and temperatures 1-3 were calculated with the conduction equation, equations 2 and 3 respectively

$$q" = h(T_\infty - T) \tag{2}$$

$$q" = k\frac{\Delta T}{t} \tag{3}$$

With all temperatures calculated the substrate mean temperature, TBC temperature gradient, and substrate temperature gradient were calculated and plotted. These results and their corresponding counterparts found in Bunker can be seen in Figures 3-5.

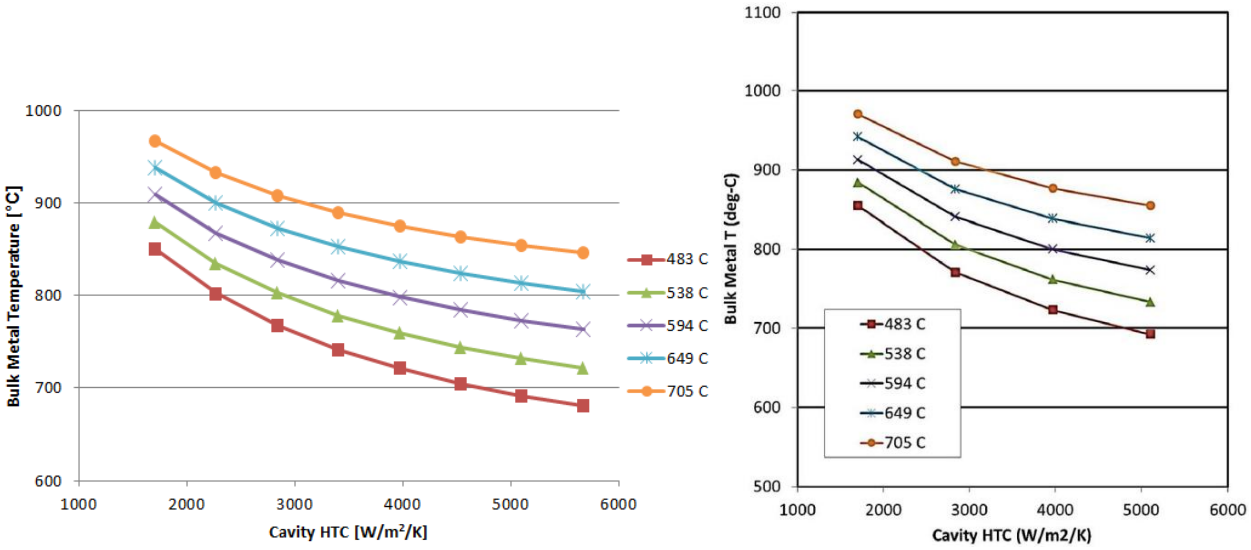

Figure 3: Calculated (left) and Bunker (right) substrate mean temperature as a function of cavity HTC and coolant temperature

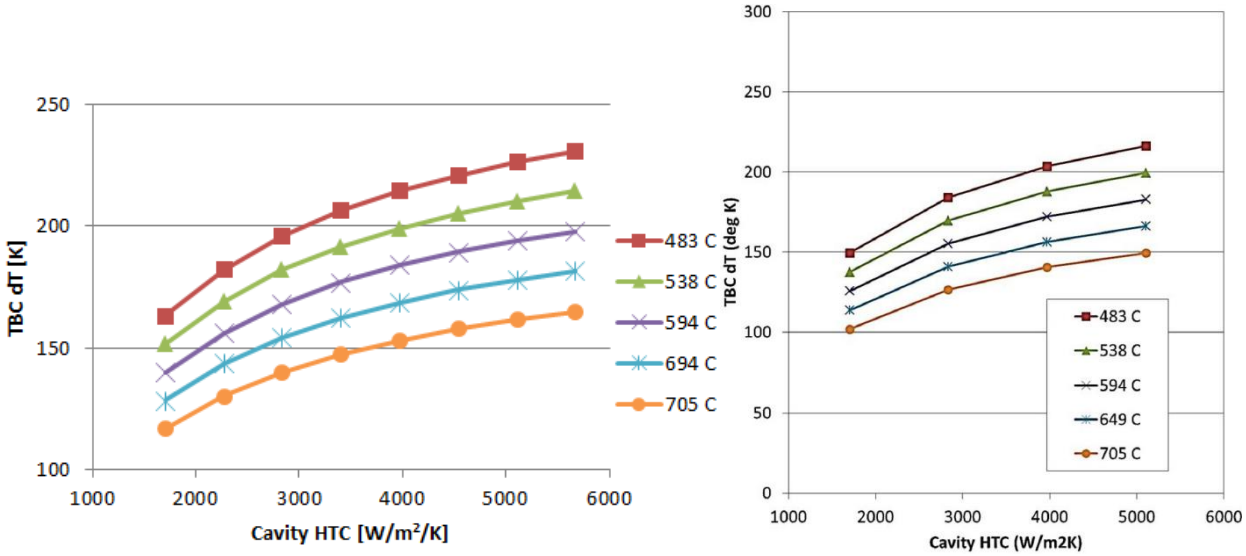

Figure 4: Calculated (left) and Bunker (right) TBC temperature gradient as a function of cavity HTC and coolant temperature

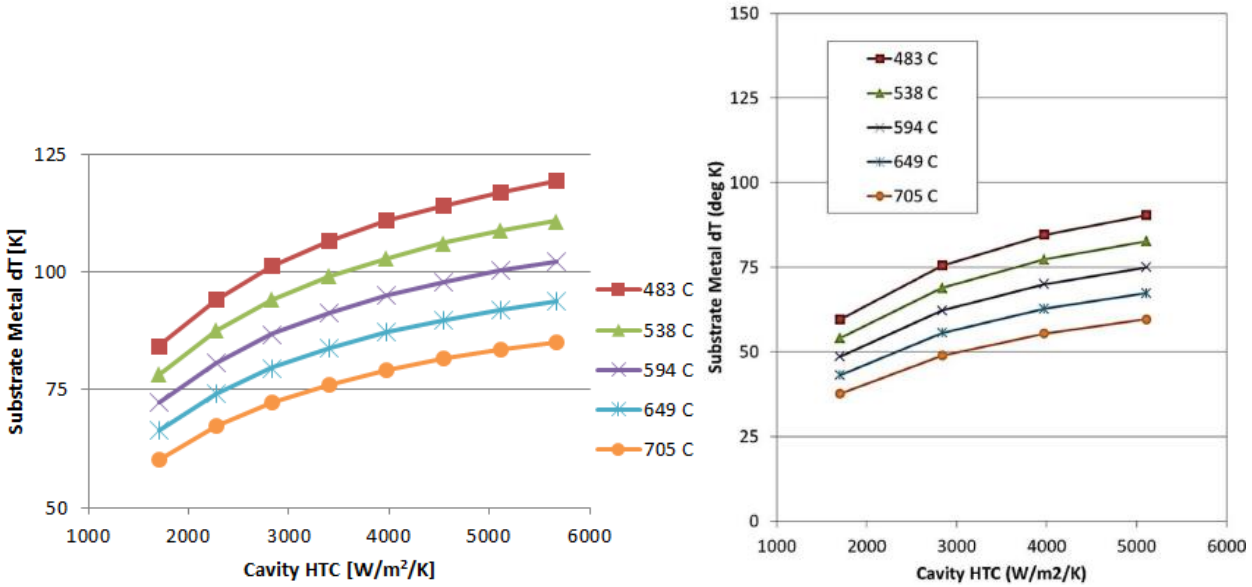

Figure 5: Calculated (left) and Bunker (right) substrate temperature gradient as a function of cavity HTC and coolant temperature

As Figure 3 shows, the substrate mean temperature decreased as the cavity HTC increased. The substrate mean temperature also decreased as the coolant temperature decreased. Figures 4 and 5 show that as the cavity HTC increased the temperature gradient across individual components of the composite wall also increased while the increase in coolant temperature caused a decrease in temperature gradient.

All of these relationships met expectations. Just as a current through individual resistors of a circuit in series is the same as the current through an equivalent single resistor, the heat flux through a composite wall in series is the same as the heat flux through each individual component of the composite wall. With this information, looking at equation 1 shows that a

higher coolant heat transfer coefficient will result in a higher heat flux. A high transfer of heat per unit area can then physically be represented by a lower mean temperature. Again looking at equation 1, a smaller coolant temperature also results in a higher heat flux leading to the same result. Looking at equations 2 and 3, a higher heat flux will result in a larger temperature gradient across a single component of a composite wall.

Taking a close look at the sets of data presented in Figures 3-5, numerical differences can be found between the calculated results and the results found in Bunker. Reasonable, numerical approximations for the results from Bunker were extracted from the plots using an online plot digitizer. Percent errors were calculated to quantify these differences. The percent errors ranged from 0-0.56% for the substrate mean temperature, 4.21-14.46% for the TBC temperature gradient, and 29.42-60.25% for the substrate metal temperature gradient.

Micro Cooling

The analysis for the micro cooling was performed using ANSYS Mechanical APDL and post processing occurred in MATLAB. The appropriate geometry was drawn up and the material thermal conductivities were applied. A mesh was automatically generated using the mesh tool as seen in Figure 6.

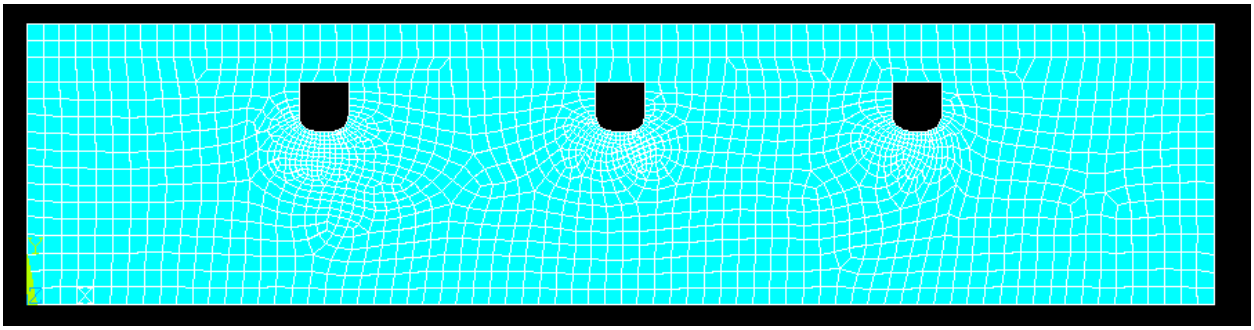

Figure 6: Meshed geometry for the micro cooling heat transfer analysis inside of ANSYS Mechanical APDL

The appropriate boundary conditions were then set as defined by Bunker. The left and right vertical walls were insulated so a zero heat flux condition was set on these walls. Convective conditions were then set on all other walls. The top wall was loaded with a bulk temperature of 1533 K and a heat transfer coefficient of 2837 W/m^2/K. The bottom wall was loaded at 756K for the bulk temperature and a varying heat transfer coefficient. The channel walls were loaded with varying bulk temperature and heat transfer coefficient. The values for the varying parameters are presented below in Table 1.

Table 1: Varying convective boundary conditions for the cavity and coolant channels

Coolant HTC (W/m^2/K)	1720	2270	2837	3405	3972	4540	5107	5675
Coolant Temperature (K)	756		811		867		922	978
Cavity HTC (W/m^2/K)	156		284		567		1135	

With these varying parameters, 136 different cases were solved to determine the temperature distribution of the geometry. Figures 7-10 present the substrate mean temperature and the temperature gradients of the TBC and substrate. The effect each parameter listed in Table 1 had on the heat transfer of the micro cooling geometry can be seen in these figures.

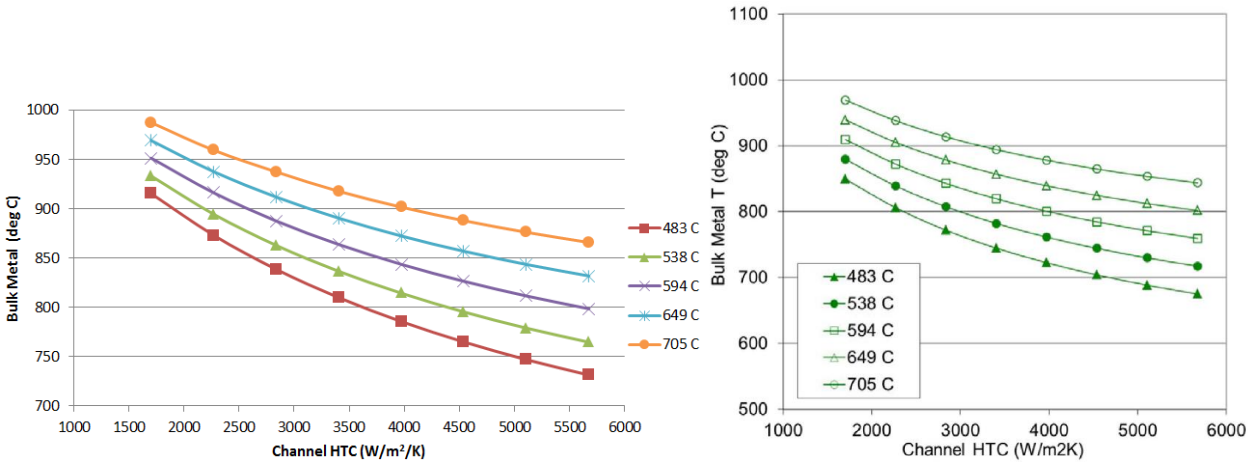

Figure 7: Calculated (left) and Bunker (right) substrate mean temperature as a function of coolant temperature and channel HTC with a constant cavity HTC of 284 W/m^2/K

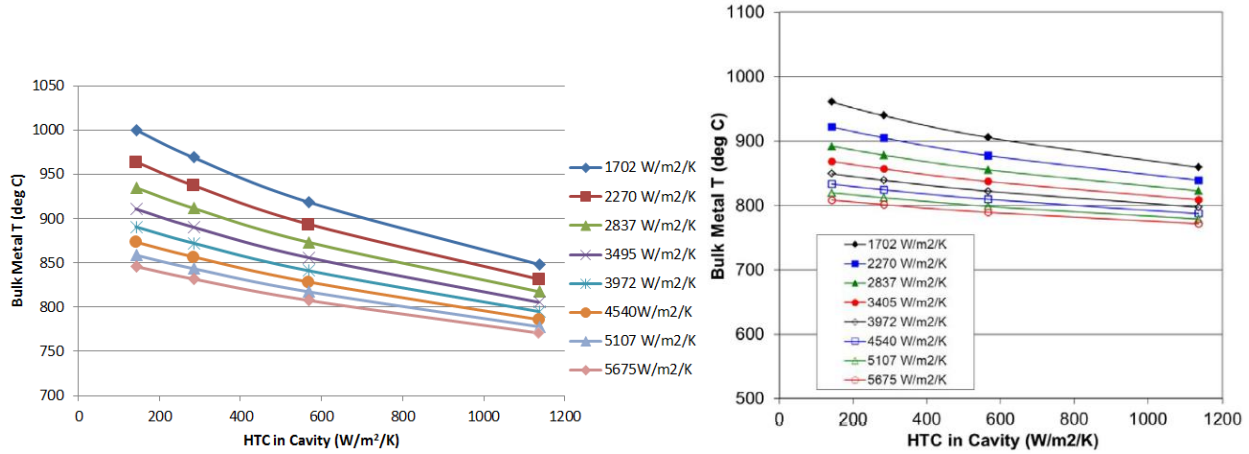

Figure 8: Calculated (left) and Bunker (right substrate mean temperature as a function of channel HTC and cavity HTC with a constant coolant temperature of 922 K

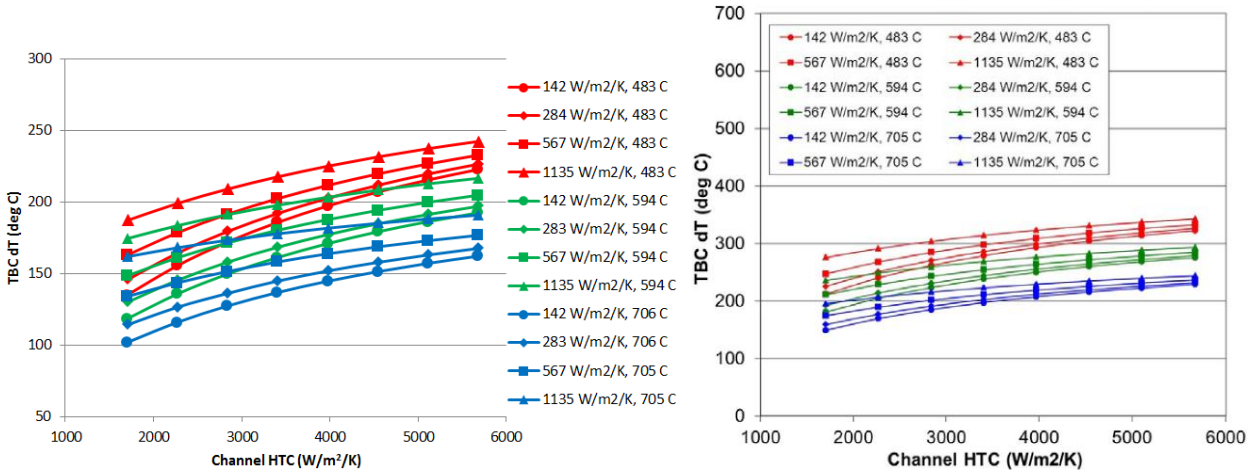

Figure 9: Calculated (left) and Bunker (right) TBC temperature gradient as a function of channel HTC, cavity HTC, and coolant temperature

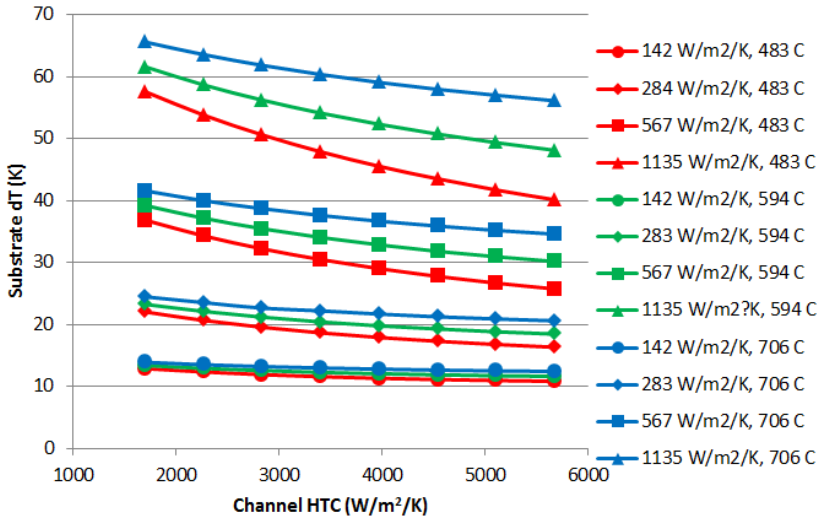

Figure 10: Calculated substrate temperature gradient as a function of channel HTC, cavity HTC, and coolant temperature

Figures 7 and 8 show the substrate mean temperature and it can be observed that a higher HTC, in either the channel or cavity, or a lower coolant temperature caused a lower substrate mean temperature as was the case in the bulk cooling. Figure 9 shows the effect the three parameters have on the TBC temperature gradient. As the cavity or channel HTC values increase, so too did the TBC temperature gradient. The opposite was true for the coolant temperature. Higher temperature values resulted in smaller temperature gradients. Figure 10 shows the resulting substrate temperature gradient. As the cavity HTC or coolant temperature increased, so too did the substrate temperature gradient. As the channel HTC increased, the substrate temperature gradient decreased.

Comparing the calculated results to the results in Bunker once again reveal a difference. The percent errors ranged from 2.00-9.01% for the substrate mean temperature with constant cavity HTC, 0.20-4.89% for the substrate mean temperature with constant coolant temperature, and 16.97-36.79% for the TBC temperature gradient.

Comparing the micro cooling results to the bulk cooling shows differences between the two cooling schemes, the most notable being the temperature gradient in the substrate metal.

With bulk cooling, the substrate temperature gradient ranged from 60.25-119.31 K. This was up to 1.8 times the maximum temperature gradient present from micro cooling which ranged from 10.87-65.57 K. Bunker presented the substrate temperature gradient from bulk cooling to be approximately 2.3 times the maximum of the micro cooling by calculating temperature gradients no larger than 39 K for the micro cooling scheme and up to 90.4 K from bulk cooling.

Coolant Savings

The final portion of Bunker's paper looked at the internal flow to calculate any coolant savings. The variable definitions for the problem can be seen in Table 2.

Table 2: Given variable definitions for coolant savings

	Micro Cooling	Bulk Cooling
Channel D	0.762 mm	2.54 cm
Blade Height	15.24 cm	15.24 cm
3-Pass Axial Length	7.62 cm	7.62 cm
Ext. Surface Area	232.3 cm^2	232.3 cm^2
Channel Spacing/D	6	n/a
Channel Length	2.54 cm	50.8 cm
Number of Channels	200	1
Coolant Inlet T	483 C	483 C
Channel Re	12500	100000
Ave. Coolant T	608 C	608 C
Coolant P	20.4 bar	20.4 bar

Using an online calculator, air properties at 608 °C and 20.4 bar were found and used for the following calculations. With the given Reynold's number and channel diameter, the coolant velocity could be calculated using equation 4

$$u = \frac{\nu Re}{D} \tag{4}$$

The velocity was found to be 82.0 and 19.7 m/s for micro and bulk cooling respectively. The difference with respect to Bunker has been attributed to possibly different air property values at the given condition. This difference was present in subsequent calculations leading to small differences due to the same reason. With the coolant velocity, the coolant mass flow rate could be calculated using equation 5

$$\dot{m} = \rho u A n \tag{5}$$

where n is the number of cooling channels. The flow rates were found to be 0.072 and 0.096 kg/s for the micro and bulk cooling respectively. The Nusselt number was calculated using equation 6, the given Reynold's number, and the Prandtl number obtained from the air properties

$$Nu = 0.23 Re^{0.8} Pr^{0.4} \tag{6}$$

The Nusselt number was found to be 38.3 and 505.3 for micro and bulk cooling respectively. With the Nusselt number calculated, the heat transfer coefficient was found to be 3111 and 1231 for the micro and bulk cooling respectively using equation 7

$$HTC = \frac{kNu}{D} \tag{7}$$

Unlike previous values, these Nusselt values resulted in much larger differences compared to Bunker yielding a percent error of 43% for both cooling cases. This difference in HTC was what prompted the review of Bunker.

Conclusion

Without access to the actual calculations Bunker performed, it was difficult if not entirely impossible to make any conclusions about the validity of the numbers presented. Even though many intermediate values were different, many of the conclusions in Bunker matched the conclusions that could be made as a result of the calculations performed. In general, micro cooling does improve cooling of turbine components. From the calculations, it was found that substrate thermal stresses were reduced by up to 45%. Coolant mass flow rates could also be reduced by up to 25%. Both of these results in turn could then allow for room to improve the overall thermal efficiency and power output of modern gas turbines.

Acknowledgement

I would like to thank the UTSR program of the Southwest Research Institute for offering the Gas Turbine Industrial Fellowship and selecting me for this opportunity. I would also like to thank Siemens Energy for sponsoring and hosting me for the summer. Special thanks go out to all of the people I was able to meet and work with for being so welcoming and helpful. This fellowship has taught me much more than I could have hoped, especially technical concepts related to the gas turbine industry and topics related to my professional development as an engineer.

References

[1] Siemens, Power and Gas. (2017, February 6). Siemens achieves breakthrough with 3D printed gas turbine blades [Press release]. Retrieved August 1, 2017, from https://www.siemens.com/press/en/pressrelease/?press=/en/pressrelease/2017/power-gas/pr2017020154pgen.htm

[2] Siemens, Power and Gas. (2017, May 22). Siemens wins 3D Printing Industry Award [Press release]. Retrieved July 31, 2017, from https://www.siemens.com/press/en/pressrelease/?press=/en/pressrelease/2017/power-gas/pr2017050308pgen.htm

[2] Bunker RS. “Gas Turbine Cooling: Moving From Macro to Micro Cooling”. ASME. Turbo Expo: Power for Land, Sea, and Air, Volume 3C: Heat Transfer ():V03CT14A002. doi:10.1115/GT2013-94277.